Supporting Information

Recognition sites effects on turn off fluorescence detection of Fe^{3+}

Senlin Li,[a] Yanan Gu,[a] Bo Zhao,[a] Haocheng Cai,[a] Zhuo Zhao,[a] Qiaozhen Sun,[*a] Bingguang Zhang[*b]

[a]*School of Materials Science and Engineering, Central South University, Changsha, 410083, China*

[b]*Key Laboratory of Catalysis and Materials Sciences of the State Ethnic Affairs Commission & Ministry of Education, College of Chemistry and Material Science, South-Central University for Nationalities, Wuhan, 430074, China*

Email: rosesunqz@csu.edu.cn (Q.-Z. Sun); 3092809@mail.scuec.edu.cn (B.-G. Zhang)

Contents

Section 1 General characterizations and structural information

Table S1 Selected Bond Lengths (Å) and Bond Angles (°) for **1** and **2**

1			
Cd(1)-N(2)	2.278(3)	Cd(1)-O(2)	2.286(3)
Cd(1)-N(4)#1	2.290(3)	Cd(1)-O(4)	2.340(3)
Cd(1)-O(5)	2.367(3)	Cd(1)-O(1)	2.490(3)
Continue			
N(2)-Cd(1)-O(2)	144.27(11)	N(2)-Cd(1)-N(4)#1	93.02(11)
O(2)-Cd(1)-N(4)#1	93.32(12)	N(2)-Cd(1)-O(4)	92.67(11)
O(2)-Cd(1)-O(4)	98.86(12)	N(4)#1-Cd(1)-O(4)	150.33(11)
N(2)-Cd(1)-O(5)	112.37(12)	O(2)-Cd(1)-O(5)	101.91(11)
N(4)#1-Cd(1)-O(5)	95.74(11)	O(4)-Cd(1)-O(5)	55.36(10)
N(2)-Cd(1)-O(1)	90.14(10)	O(2)-Cd(1)-O(1)	54.16(9)
N(4)#1-Cd(1)-O(1)	97.45(11)	O(4)-Cd(1)-O(1)	111.63(10)
O(5)-Cd(1)-O(1)	153.19(11)		
2			
Cd(1)-O(10)#1	2.261(3)	Cd(1)-O(9)	2.265(3)
Cd(1)-O(3)	2.279(3)	Cd(1)-N(3)	2.318(3)
Cd(1)-N(2)	2.345(3)	Cd(1)-O(2)	2.530(3)
Cd(2)-O(4)	2.313(3)	Cd(2)-N(4)	2.336(3)
Cd(2)-N(5)	2.341(3)	Cd(2)-O(5)#2	2.338(3)
Cd(2)-O(7)#3	2.373(3)	Cd(2)-O(8)#3	2.383(3)
O(10)#1-Cd(1)-O(9)	117.21(10)	O(10)#1-Cd(1)-O(3)	95.54(11)
O(9)-Cd(1)-O(3)	86.80(10)	O(10)#1-Cd(1)-N(3)	89.56(12)
O(9)-Cd(1)-N(3)	89.51(11)	O(3)-Cd(1)-N(3)	174.67(11)
O(10)#1-Cd(1)-N(2)	140.90(12)	O(9)-Cd(1)-N(2)	96.81(10)
O(3)-Cd(1)-N(2)	105.59(11)	N(3)-Cd(1)-N(2)	71.02(12)
O(10)#1-Cd(1)-O(2)	83.39(10)	O(9)-Cd(1)-O(2)	138.62(10)
O(3)-Cd(1)-O(2)	54.20(9)	N(3)-Cd(1)-O(2)	128.24(10)
N(2)-Cd(1)-O(2)	82.99(10)	O(4)-Cd(2)-N(4)	90.81(11)
O(4)-Cd(2)-N(5)	84.05(11)	N(4)-Cd(2)-N(5)	70.17(12)
O(4)-Cd(2)-O(5)#2	126.31(10)	N(4)-Cd(2)-O(5)#2	88.60(12)
N(5)-Cd(2)-O(5)#2	143.97(11)	O(4)-Cd(2)-O(7)#3	83.66(10)
N(4)-Cd(2)-O(7)#3	170.50(12)	N(5)-Cd(2)-O(7)#3	101.48(12)
O(5)#2-Cd(2)-O(7)#3	100.89(11)	O(4)-Cd(2)-O(8)#3	134.07(11)
N(4)-Cd(2)-O(8)#3	127.39(11)	N(5)-Cd(2)-O(8)#3	86.48(11)
O(5)#2-Cd(2)-O(8)#3	83.94(11)	O(7)#3-Cd(2)-O(8)#3	54.53(10)

Symmetry codes: for **1**: -x+1/2, y+1/2, -z-1/2; for **2**: #1: -x, -y, -z+1; #2: -x+1, -y, -z+2; #3: x+1, y, z+1.

Table S2 Hydrogen bond distances (Å) and bond angles (°) for **1** and **2**

D-H⋯A	d(D-H)	d(H…A)	d(D…A)	∠(DHA)
1				
OW(1)-HW(1C)…O(4)#1	0.85	2.11	2.953(5)	172
OW(1)-HW(1D)…OW(3)#2	0.85	2.01	2.855(10)	174
N(3)-H(3A)…OW3	0.86	2.08	2.886(8)	156
N(3)-H(3A)…OW3'	0.86	2.06	2.915(12)	173
C(11)-H (11A)…O(2)#3	0.96	2.48	3.352(5)	150
C(15)-H (15A)…O(4)#1	0.93	2.56	3.256(4)	132
2				
C(1)-H(1A)…O(8)#1	0.93	2.35	3.273(5)	173
C(9)-H(9A)…O(3)#2	0.93	2.49	3.370(6)	152
C(21)-H(21A)…O(3)#1	0.93	2.52	3.353(6)	149
C(22)-H(22A)…O(7)#1	0.93	2.42	3.253(6)	149
C(25)-H(25A)…O(2)#3	0.93	2.57	3.374(5)	145
C(32)-H(32A)…O(2)#1	0.93	2.44	3.371(5)	175
C(41)-H(41C)…S(1)#2	0.96	2.94	3.802(5)	151

Symmetry codes: for **1**: #1: -x+1/2, y+1/2, -z+1/2; #2: -x-1, -y, -z-1; #3: x+1, y, z; for **2**: #1: -x, -y, -z+1; #2: -x, -y-1, -z+1; #3: x+1, y, z.

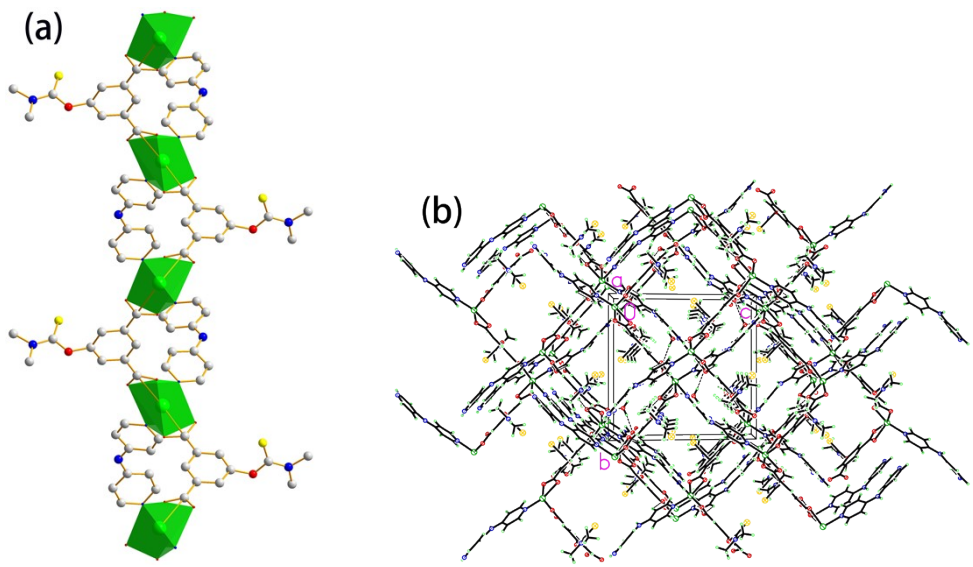

Fig. S1 (a) The two-dimensional (2D) plane of compound **1** along c axis; (b) The packing diagram of **1**. The hydrogen bonds are shown in dashed lines.

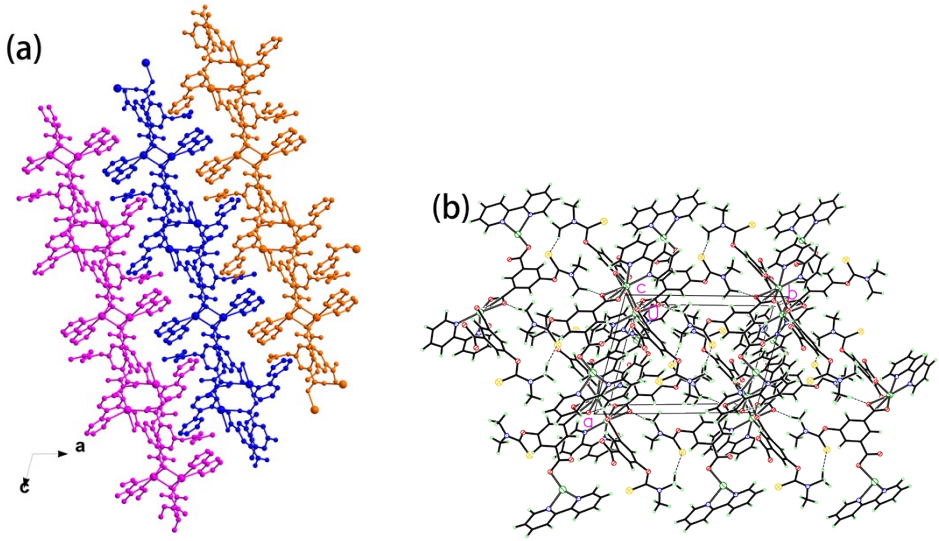

Fig. S2 (a) The neighboring chains along b axis; (b) The packing diagram of compound **2**. The hydrogen bonds are shown in dashed lines.

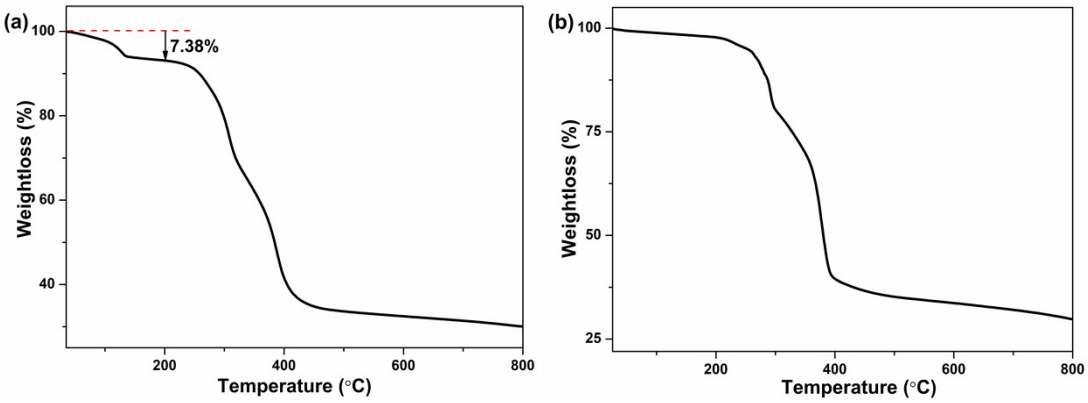

Fig. S3 The thermal analysis curve of compound **1** (a) and **2** (b).

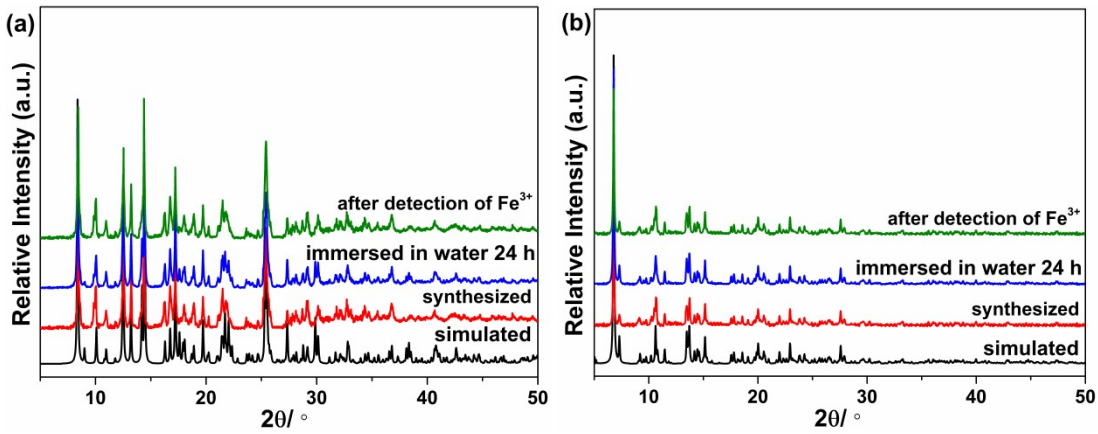

Fig. S4 PXRD pattern of compound **1** (a) and **2** (b), the immersed sample and the detection of Fe^{3+} and 4-NP.

Section 2 Detection of Fe^{3+}

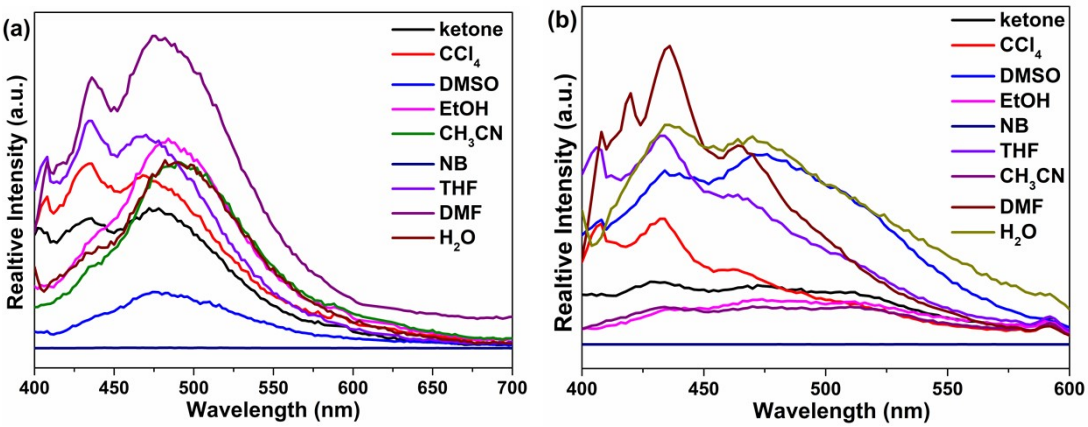

Fig. S5 Luminescent spectra of **1** (a) (λ_{ex}: 302 nm) and **2** (b) (λ_{ex}: 356 nm) in different solvents (Condition: 5 mg 1, 3 mL solvent).

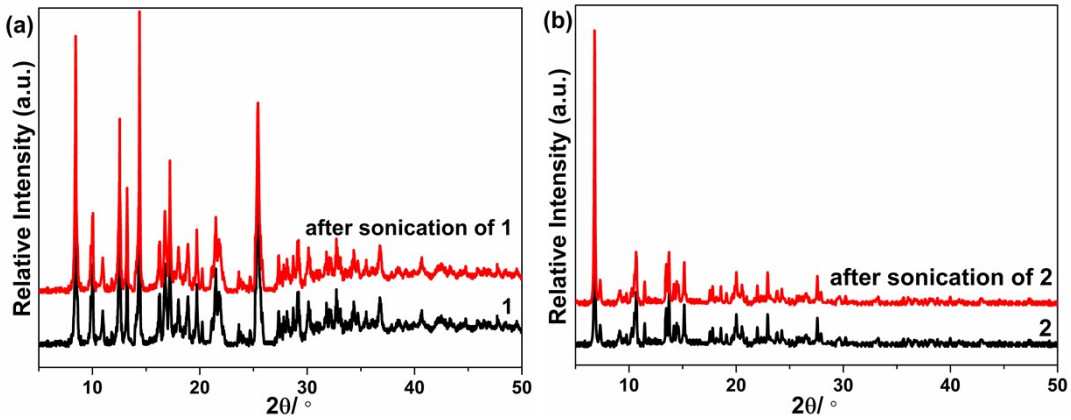

Fig. S6 PXRD pattern of compounds **1** (a) and **2** (b) before and after sonication in water.

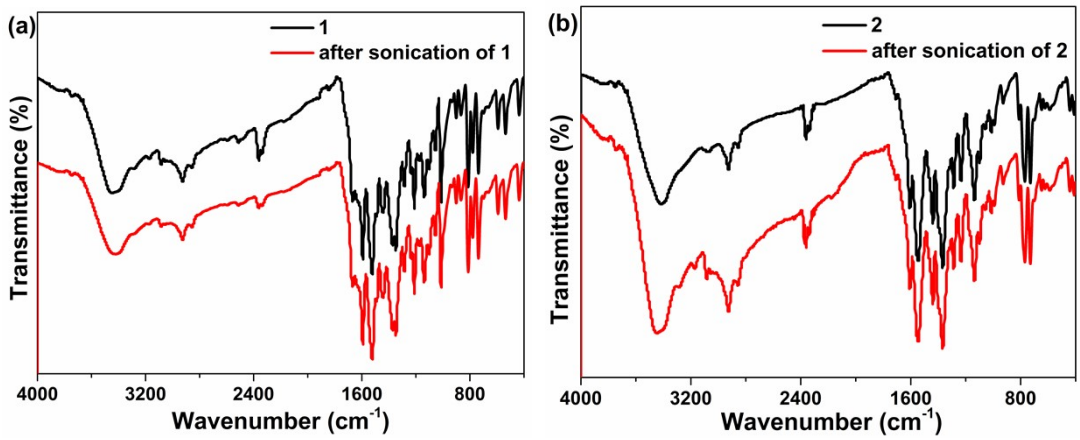

Fig. S7 IR spectra of compounds **1** (a) and **2** (b) before and after sonication in water.

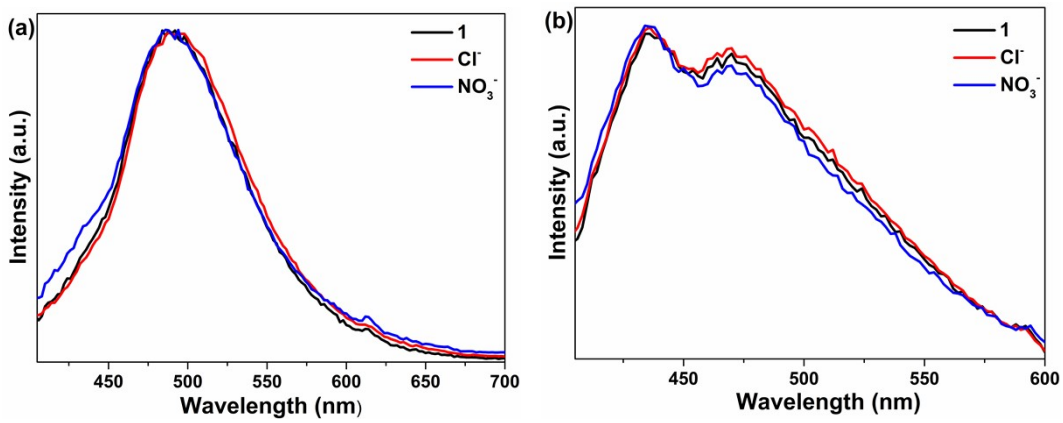

Fig. S8 The emission spectra of **1** (a) and **2** (b) immersed in water solution of NaCl and $NaNO_3$, respectively (Condition: 5 mg **1** (**2**), 3 mL H_2O and 0.02 mmol Na^+ ion).

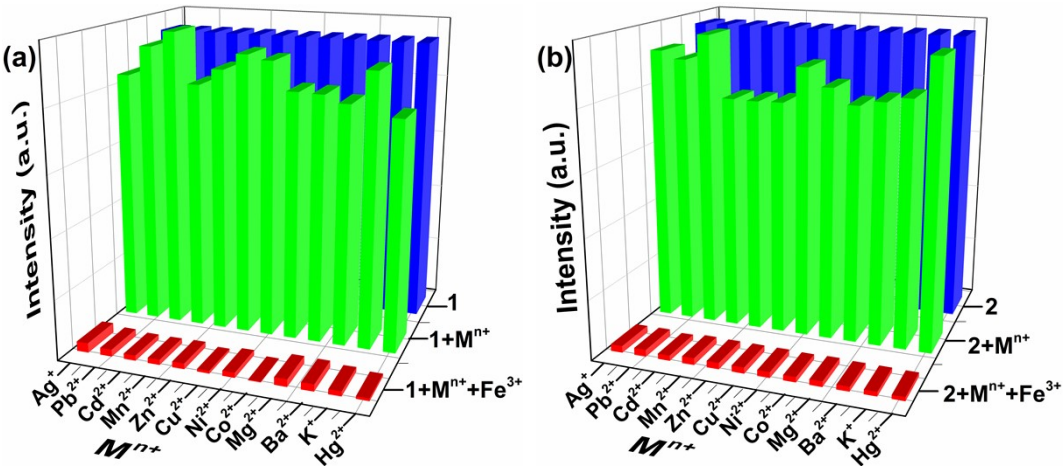

Fig. S9 The competition experiments of **1** (a) and **2** (b) for detection of Fe^{3+} ions in the presence of the interfering metal cations (Condition: 5 mg **1** (**2**), 3 mL H_2O, 10 μL M^{n+} ions (0.1 M) and 10 μL Fe^{3+} (0.01 M)).

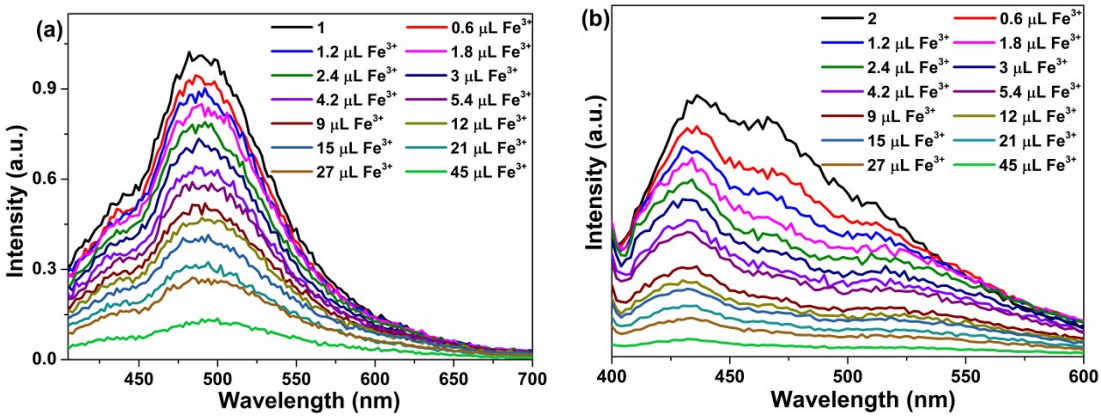

Fig. S10 Fluorescent spectra of **1** (a) and **2** (b) suspension (1.67 mg/mL) upon incremental addition of Fe^{3+} (0.01 M).

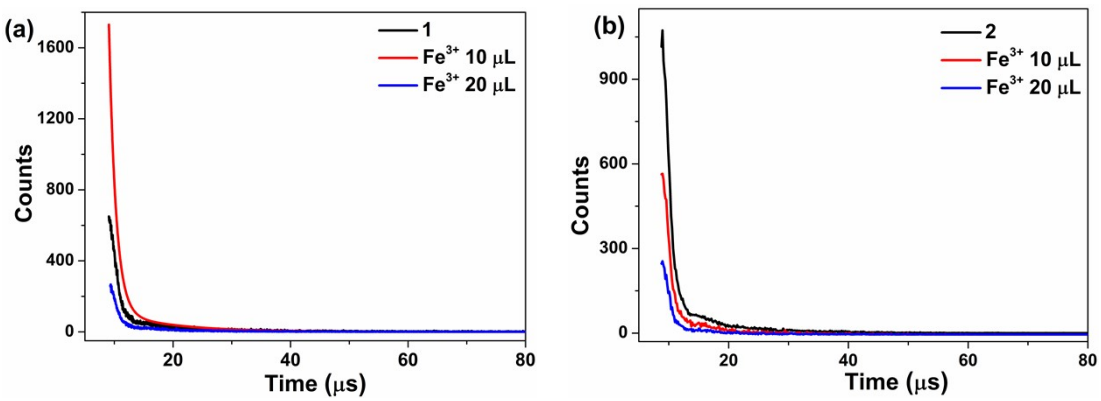

Fig. S11 The fluorescence decay curves of **1** (a) and **2** (b) in Fe^{3+} solution (0.01 M).

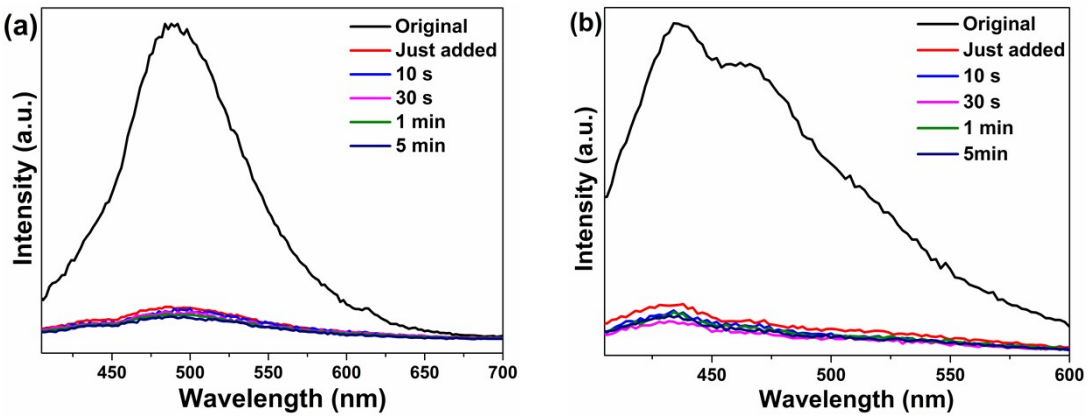

Fig. S12 Time-dependent fluorescent quenching detections of **1** (a) and **2** (b) for Fe^{3+}.

To calculate the standard deviation and detection limit of this detection method, 5 mg **1** (**2**) was well ground and suspended in 3 mL H_2O. Then, Fe^{3+} ion solution (0.01 M) was added into the suspension and the fluorescent intensities were recorded. Standard deviation (σ) was calculated from five blank tests of **1** (**2**) suspension and the detection limit was calculated via the formula: 3σ/k (k: slope of the straight line).

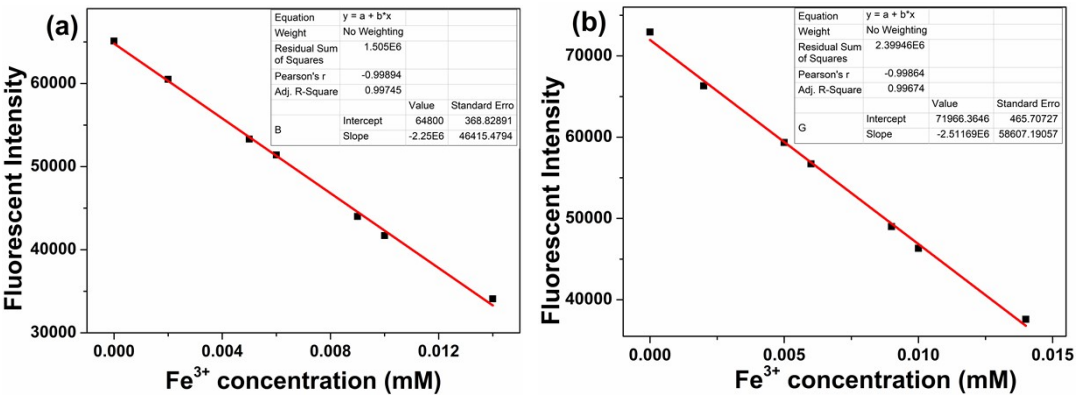

Fig. S13 Linear curve of fluorescent intensity of **1** (a) and **2** (b) suspension upon incremental addition of Fe^{3+}.

Table S3 Standard deviation calculation

	Fluorescent intensity ($\times 10^4$)
Compound **1**	
Test 1	6.510
Test 2	6.522
Test 3	6.512
Test 4	6.515
Test 5	6.518
Standard deviation (σ)	0.0048
Compound **2**	
Test 1	6.450
Test 2	6.439
Continue	
Test 3	6.446
Test 4	6.456
Test 5	6.444
Standard deviation (σ)	0.0064

Table S4 Detection limit calculation for Fe^{3+}

Compounds	
1	
Slope (k)	2.25×10^6 mM^{-1}
Detection limit (3σ/k)	6.40×10^{-5} mM
2	
Slope (k)	2.51×10^6 mM^{-1}
Detection limit (3σ/k)	7.65×10^{-5} mM

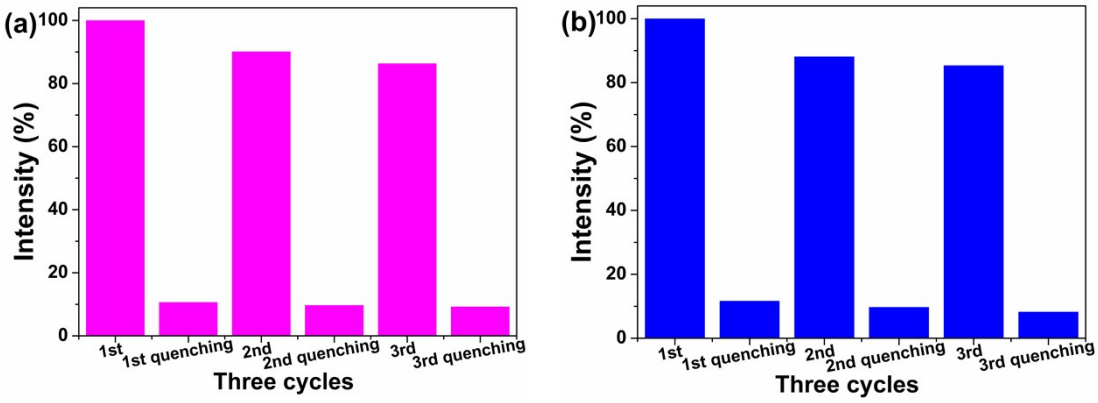

Fig. S14 Three quenching cycles of **1** (a) and **2** (b) suspension after addition of Fe^{3+}.

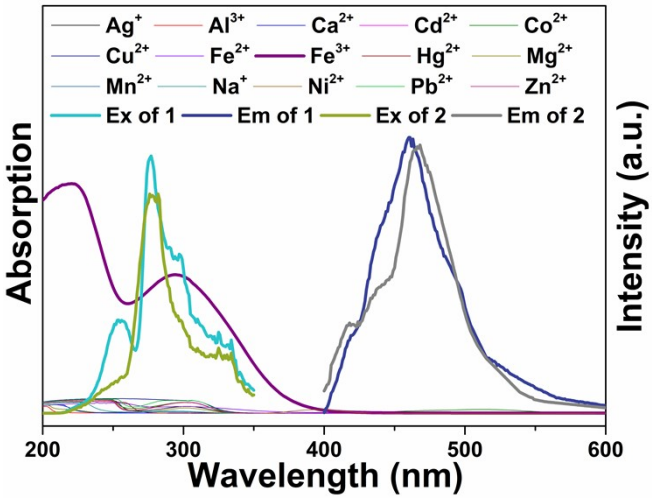

Fig. S15 UV−vis spectra of metal salts, the excitation and emission spectra of **1** and **2**, showing their overlapping.

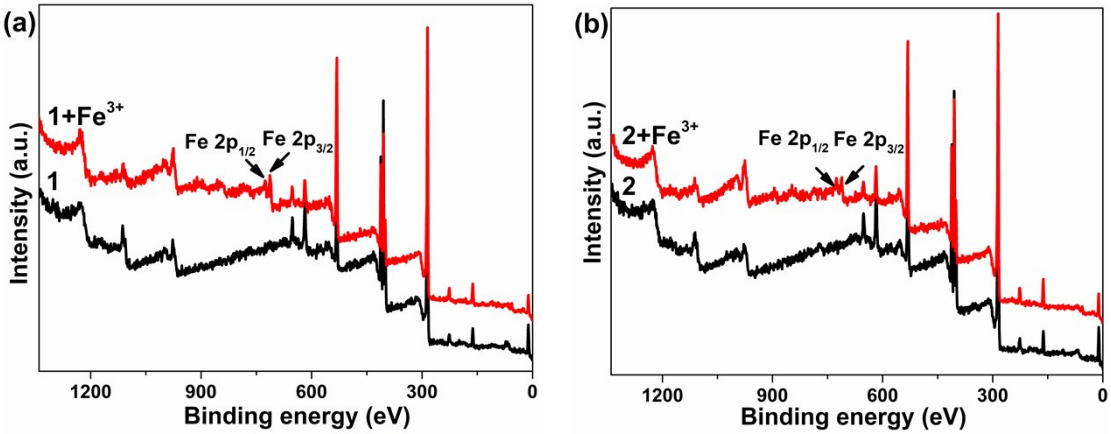

Fig. S16 XPS for compound **1** and Fe^{3+} incorporating **1** (a), **2** and Fe^{3+} incorporating **2**.

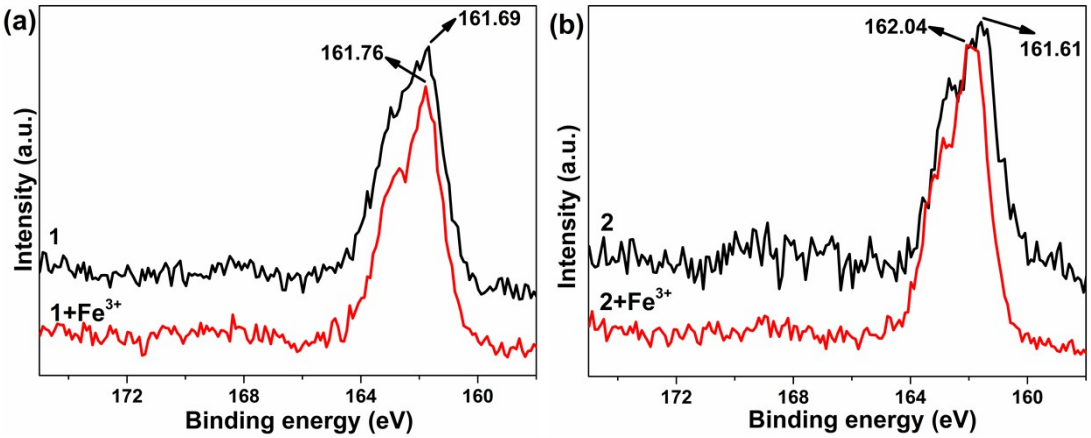

Fig. S17 S 2p XPS for **1** and Fe^{3+} incorporating **1** (a), **2** and Fe^{3+} incorporating **2** (b).

Table S5 The comparison of XPS peak-peak displacement values in **1** and **2**

1			**2**	
$\Delta E_{pyridine}$	ΔE_{amine}	$\Delta E_{dimethylamino}$	$\Delta E_{pyridine}$	$\Delta E_{dimethylamino}$

N 1s	0.21	0.49	0.06	0.30	0.58
	ΔE_{alkyl}	$\Delta E_{carboxyl}$		ΔE_{alkyl}	$\Delta E_{carboxyl}$
O 1s	0.14	0.29		0.32	0.47
	ΔE			ΔE	
S 2p	0.07			0.43	

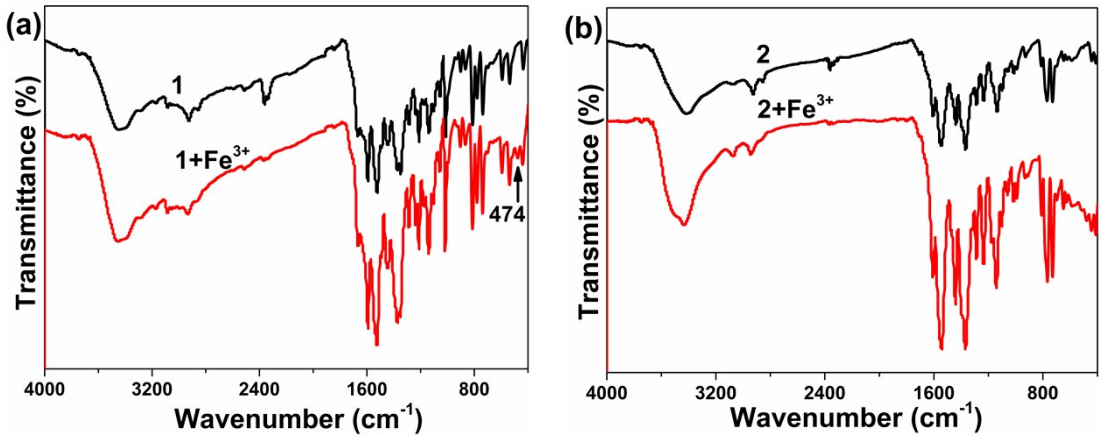

Fig. S18 (a) FT-IR spectra for compound **1** and Fe^{3+} incorporated **1**; (b) FT-IR spectra for compound **2** and Fe^{3+} incorporated **2**.